

OPTIMAL FILTERING OF STOCHASTIC DISTURBANCES FOR CORIOLIS VIBRATORY GYROSCOPES

Introduction

Significant amount of interest received by Coriolis vibratory gyroscopes (CVGs) from the both scientific and engineering communities is due to the possibility to fabricate sensitive elements of such gyroscopes in miniature form by using modern microelectronic mass-production technologies. Such gyroscopes are frequently referred to as MEMS (Micro-Electro-Mechanical-Systems) gyroscopes. Being based on sensing of Coriolis acceleration due to the rotation in oscillating structures, CVGs have a lot more complicated mathematical models, comparing to the conventional types of gyroscopes. One of such complication is a result of the useful signal proportional to the external angular rate being modulated with the intentionally excited primary oscillations [1–3]. From the control systems point of view, conventional representation of CVGs incorporates primary oscillation excitation signal as an input to the dynamic system, and unknown angular rate as a coefficients of its transfer functions [3]. As a result, conventional control and filtering systems design is practically impossible. At the same time, performances of CVGs are limited mainly due to the low signal-to-noise ratios. In view of this problem, optimal noise filter development is highly necessary. The latter could be achieved only in systems where unknown angular rate is no longer a system parameter but its input.

This paper briefly describes newly developed method of CVG dynamics analysis by means of complex amplitude-phase variables, which enables conventional optimal filter design, as well as a static optimal filter synthesis for process noise in CVGs.

Problem formulation

In order to be able to synthesise optimal filters for CVGs the following major steps must be completed: a) development of the mathematical model in demodulated signals, b) obtaining system transfer functions where angular rate is an input, c) analysis of stochastic disturbances affecting performances of CVGs, d) synthesis of optimal filters based on the obtained earlier transfer functions with respect to the spectral characteristics of stochastic disturbances,

and finally e) numerical simulations proving the performances of the optimal filters.

Demodulated dynamics of Coriolis vibratory gyroscopes

In the most generalized form, motion equations of the CVG sensitive element both with translational and rotational motion could be represented in the following form [4]:

$$\begin{cases} \ddot{x}_1 + 2\zeta_1 k_1 \dot{x}_1 + (k_1^2 - d_1 \Omega^2)x_1 + g_1 \Omega \dot{x}_2 + d_3 \dot{\Omega} x_2 = q_1(t), \\ \ddot{x}_2 + 2\zeta_2 k_2 \dot{x}_2 + (k_2^2 - d_2 \Omega^2)x_2 - g_2 \Omega \dot{x}_1 - \dot{\Omega} x_1 = q_2(t). \end{cases} \quad (1)$$

Here x_1 and x_2 are the generalized coordinates that describe primary (excited) and secondary (sensed) motions of the sensitive element respectively, k_1 and k_2 are the corresponding natural frequencies, ζ_1 and ζ_2 are the dimensionless relative damping coefficients, Ω is the measured angular rate, which is orthogonal to the axes of primary and secondary motions, q_1 and q_2 are the generalized accelerations due to the external forces acting on the sensitive element. The remaining dimensionless coefficients are different for the sensitive elements exploiting either translational or rotational motion. For the translational sensitive element they are $d_1 = d_2 = 1$, $d_3 = m_2 / (m_1 + m_2)$, $g_1 = 2m_2 / (m_1 + m_2)$, $g_2 = 2$, where m_1 and m_2 are the masses of the outer frame and the internal massive element. In case of the rotational motion of the sensitive element, these coefficients are the functions of different moments of inertia (for greater details see [4]).

In order to make the equations (1) suitable for to the transfer function synthesis one must make the following assumptions: angular rate is small comparing to the primary and secondary natural frequencies so that

$$k_1^2 \gg d_1 \Omega^2, \quad k_2^2 \gg d_2 \Omega^2 \quad (2)$$

and rotational and Coriolis accelerations acting along primary oscillation axis are negligible in comparison to the accelerations from driving forces

$$g_1 \Omega \dot{x}_2 + d_3 \dot{\Omega} x_2 \ll q_1(t). \quad (3)$$

Taking into considerations assumptions (2) and (3), motions equations (1) could be simplified to the following form:

$$\begin{cases} \ddot{x}_1 + 2\zeta_1 k_1 \dot{x}_1 + k_1^2 x_1 = q_1(t), \\ \ddot{x}_2 + 2\zeta_2 k_2 \dot{x}_2 + k_2^2 x_2 = g_2 \Omega \dot{x}_1 + \dot{\Omega} x_1. \end{cases} \quad (4)$$

Here we also assumed that no external driving forces are affecting the secondary oscillations, which means that $q_2(t) = 0$. System of equations (4) is now

perfectly suitable for further transformations towards the desired representation in terms of the unknown angular rate.

Using the following amplitude–phase substitutions for primary and secondary generalized displacements of CVG sensitive element:

$$\begin{aligned} x_1(t) &= \text{Im}\{A_1(t)e^{j\omega t}\}, & A_1(t) &= A_{10}(t)e^{j\phi_{10}(t)}, \\ x_2(t) &= \text{Im}\{A_2(t)e^{j\omega t}\}, & A_2(t) &= A_{20}(t)e^{j\phi_{20}(t)}, \end{aligned}$$

where A_{10} and A_{20} are the primary and secondary oscillation amplitudes, ϕ_{10} and ϕ_{20} are the corresponding phase shifts relatively to the excitation force, motion equations (4) will become

$$\begin{cases} \ddot{A}_1 + 2(\zeta_1 k_1 + j\omega)\dot{A}_1 + (k_1^2 - \omega^2 + 2j\omega k_1 \zeta_1)A_1 = q_{10}, \\ \ddot{A}_2 + 2(\zeta_2 k_2 + j\omega)\dot{A}_2 + (k_2^2 - \omega^2 + 2j\omega k_2 \zeta_2)A_2 = (j\omega g_2 \Omega + \dot{\Omega})A_1 + g_2 \dot{A}_1 \Omega. \end{cases} \quad (5)$$

Equations (5) describe variations of the amplitude and phase of the primary and secondary equations in time with respect to the unknown non–constant angular rate $\Omega(t)$. This allows conducting analysis of the Coriolis vibratory gyroscope dynamics without constraining the angular rate to be constant or slowly varying.

Analysing system (5), one can see that the first equation can be solved separately from the second one. After homogeneous solutions of the first equation faded out, only non–homogenous solution remains. In this case, amplitude of the primary oscillations is

$$A_1 = \frac{q_{10}}{k_1^2 - \omega^2 + 2jk_1 \zeta_1 \omega}, \quad (6)$$

and it is constant in time, yielding $\ddot{A}_1 = \dot{A}_1 = 0$. Indeed, most of the time measurements of the angular rate are performed when primary oscillations have already settled. As a result, only equation for the secondary oscillations remains, in which the complex primary amplitude A_1 is just a constant parameter given by (6):

$$\ddot{A}_2 + 2(\zeta_2 k_2 + j\omega)\dot{A}_2 + (k_2^2 - \omega^2 + 2j\omega k_2 \zeta_2)A_2 = (j\omega g_2 \Omega + \dot{\Omega})A_1. \quad (7)$$

Equation (7) now describes amplitude–phase of the secondary oscillations with respect to the settled primary oscillations.

System transfer functions

Having CVG sensitive element motion equation in the form (7), allows obtaining its transfer functions from the input angular rate to the amplitude of the secondary oscillations. Application of the Laplace transformation to the

equations (7) with respect to zero initial conditions for all time-dependent variables results in the following expressions:

$$[(s + j\omega)^2 + 2\zeta_2 k_2 (s + j\omega) + k_2^2] A_2(s) = A_1[s + jg_2\omega] \Omega(s). \quad (8)$$

Solution of the algebraic equation (10) for the secondary amplitude-phase Laplace transform is

$$A_2(s) = \frac{A_1(s + jg_2\omega)}{(s + j\omega)^2 + 2\zeta_2 k_2 (s + j\omega) + k_2^2} \Omega(s). \quad (9)$$

Considering the angular rate as an input, the system transfer function for the secondary amplitude-phase is

$$\begin{aligned} W_2(s) &= \frac{A_2(s)}{\Omega(s)} = \frac{A_1(s + jg_2\omega)}{(s + j\omega)^2 + 2\zeta_2 k_2 (s + j\omega) + k_2^2} = \\ &= \frac{q_{10}(s + jg_2\omega)}{[(s + j\omega)^2 + 2\zeta_2 k_2 (s + j\omega) + k_2^2][k_1^2 - \omega^2 + 2j\omega k_1 \zeta_1]}. \end{aligned} \quad (10)$$

One should note that transfer function (10) has complex coefficients, which results in the complex system outputs as well.

There is quite an important special case, when complex transfer function (10) transform to the simple real-valued one. Assuming equal primary and secondary natural frequencies ($k_1 = k_2 = k$), equal damping ratios ($\zeta_1 = \zeta_2 = \zeta$), resonance excitation ($\omega = k$), and constant angular rate, one can easily obtain

$$W_{20}(s) = \frac{A_{20}(s)}{\Omega(s)} = \frac{q_{10}g_2}{4k^2\zeta(s + k\zeta)}. \quad (11)$$

Transfer function (11) relates angular rate to the secondary oscillations amplitude. However, more appropriate would be to consider transfer function relating unknown input angular rate to the measured angular rate, which can be easily obtained from (11) by dividing it on the steady state scale factor. The resulting transfer function is

$$W_{\Omega}(s) = \frac{k\zeta}{s + k\zeta}. \quad (12)$$

Although this case appears to be very specific, it still approximates transient process of a “tuned” CVG with accuracy suitable for most of applications [6, 7].

Stochastic disturbances

Performances of CVGs can be affected by uncontrolled stochastic influences in two ways: as a “sensor noise”, which is added to the output of the system, and as a “process noise” or disturbances, which are added to the input of the system. The latter could be also treated as “rate-like” disturbances. Such system is shown in the figure 1.

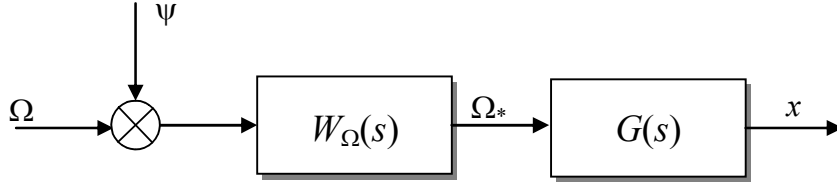


Fig. 1. CVG with added “rate-like” disturbances

Here $W_{\Omega}(s)$ is the system transfer function given by (12), ψ is the stochastic disturbance, Ω is the angular rate, $G(s)$ is the optimal filter yet to be developed, x is the filtered output of the system, which in ideal case is equal to the angular rate Ω .

Looking at the system in the figure 1, one can see that the only way to separate output resulting from the angular rate, from the output generated by the disturbances ψ is to take into account additional information about angular rate and disturbances. Assuming that CVG is installed on a moveable object, such as aircraft or land vehicle, its power spectral density can be represented as

$$S_{\Omega}(s) = \frac{\sigma^2 B^2}{B^2 - s^2}, \quad (13)$$

where B is the moveable object bandwidth. In this case disturbances can be represented by the white noise as follows

$$S_{\psi}(s) = \gamma^2 \sigma^2. \quad (14)$$

Here γ is the disturbance to angular rate ratio (“noise-to-signal” ratio). While using white noise as a model of disturbances is quite common, the synthesised filter may not perform as good as expected due to the fact, that we suggest disturbances to be present within the object bandwidth. This situation can be resolved by using high-pass disturbances adjacent to the object bandwidth. The corresponding power spectral density is

$$S_{\psi}(s) = -\frac{\gamma^2 \sigma^2 s^2}{B^2 - s^2}. \quad (15)$$

Power spectral densities (14) and (15) cover most of the present in CVG cases of stochastic disturbances.

Optimal filter synthesis algorithm

The problem of optimal filter synthesis is formulated and solved for the system shown in Fig. 2 below [8], with respect to the stationary stochastic sensor noise. In the most general case, $W(s)$ is the matrix of sensor transfer functions, $G(s)$ is the matrix of filter transfer functions, φ is the noise vector, r is

the input vector, which then is measured by the sensor, and x is the system output vector, which in our case is an estimation of the input.

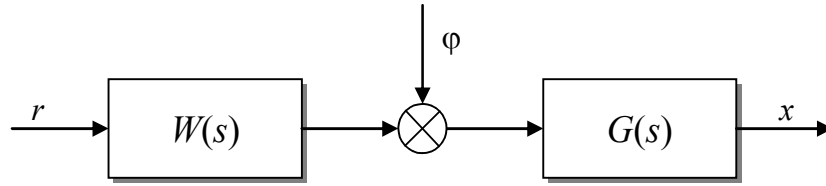


Fig. 2. Optimal noise filtering

Error of this system is defined as a difference between the actual output of the system x and the ideal output, which is the given desired transformation $H(s)$ of the input:

$$\varepsilon = x - H(s) \cdot r .$$

It is also assumed that signals x and r are the centred stochastic processes with known spectral densities $S_{rr}(s)$, $S_{\phi\phi}(s)$, $S_{r\phi}(s)$, and $S_{\phi r}(s)$.

Performance criterion for the system is assumed in the following form:

$$J = E\{\varepsilon' \cdot R \cdot \varepsilon\} = \frac{1}{j} \int_{-j\infty}^{j\infty} \text{tr}(S'_{\varepsilon\varepsilon} \cdot R) ds . \quad (16)$$

Here R is the weight matrix, and $S'_{\varepsilon\varepsilon}(s)$ is the transposed matrix of the error spectral densities. Using Wiener–Khinchin theorem we can calculate the error spectral density from the system transfer functions and signal spectral densities as follows:

$$\begin{aligned} S'_{\varepsilon\varepsilon}(s) = & (GW - H)S'_{rr}(W_*G_* - H_*) + (GW - H)S'_{\phi r}G_* \\ & + GS'_{r\phi}(W_*G_* - H_*) + GS'_{\phi\phi}G_* , \end{aligned} \quad (17)$$

where “*” designates Hermite conjugate. By means of introducing new variables defined as

$$\begin{aligned} DD_* = & WS'_{rr}W_* + WS'_{\phi r} + S'_{r\phi}W_* + S'_{\phi\phi} , \\ \Gamma\Gamma_* = & R , \quad G_0 = \Gamma GD , \end{aligned} \quad (18)$$

$$T = \Gamma H(S'_{rr}W_* + S'_{\phi r})D_*^{-1} ,$$

and substituting power spectral density (17) into (16), first variation of the performance criterion (16) with respect to the unknown filter related function G_0 will be

$$\delta J = \frac{1}{j} \int_{-j\infty}^{j\infty} \text{tr}[(G_0 - T)\delta G_0 + \delta G_{0*}(G_{0*} - T_*)] ds. \quad (19)$$

Minimum of the performance criterion is achieved when first variation (19) is zero. Apparently, this is achieved when

$$G = \Gamma^{-1}(T_0 + T_+)D^{-1}. \quad (20)$$

Here T_0 is the integral part of the matrix T , and T_+ is the part of the matrix T that contains only poles with negative imaginary part. These matrices are the result of the Wiener separation procedure.

For the case of stochastic disturbances, power spectral density $S_{rr}(s)$ corresponds to (13), and spectral density $S_{\phi\phi}(s)$ can be calculated from (14) using Wiener–Khinchin theorem as follows:

$$S_{\phi\phi}(s) = |W_{\Omega}(s)|^2 S_{\psi}(s) = \frac{\gamma^2 \sigma^2 k^2 \zeta^2}{-s^2 + k^2 \zeta^2}, \quad (21)$$

and in case of the high-pass disturbances (15)

$$S_{\phi\phi}(s) = \frac{\gamma^2 \sigma^2 k^2 \zeta^2 s^2}{(-s^2 + k^2 \zeta^2)(-s^2 + B^2)}. \quad (22)$$

If fact, expressions (21) and (22) obtained by transforming system in Fig. 1 to the system presented in Fig. 2.

Spectral densities (21) and (22) along with the suggested angular rate spectral density can now be used to derive optimal filters based on the formula (20). After performing transformations according to (18), the optimal filters are found as:

$$G(s) = \frac{B\sqrt{1+\gamma^2}(s+\zeta k)}{\zeta k(\gamma s + B\sqrt{1+\gamma^2})}, \quad (23)$$

in case of the “white-noise” disturbances and

$$G(s) = \frac{B(s + \zeta k)}{\zeta k(B + \gamma s)}, \quad (24)$$

in case of the “high-pass” disturbances. Depending on which of the disturbance model is found to be the most appropriate, either filter (23) or filter (24) should be used.

Let us now study performances of the obtained optimal filters (23) and (24) in numerical simulations of the realistic CVG.

Numerical simulations

In order to obtain the most realistic simulation results, equations (1) were used to build a numerical model of CVG dynamics using Simulink/Matlab. Resulting sensitive element model is shown in the figure 3.

In this model centrifugical accelerations were neglected according to (2) and synchronous demodulator is added. Input angular rate is assumed to be a constant.

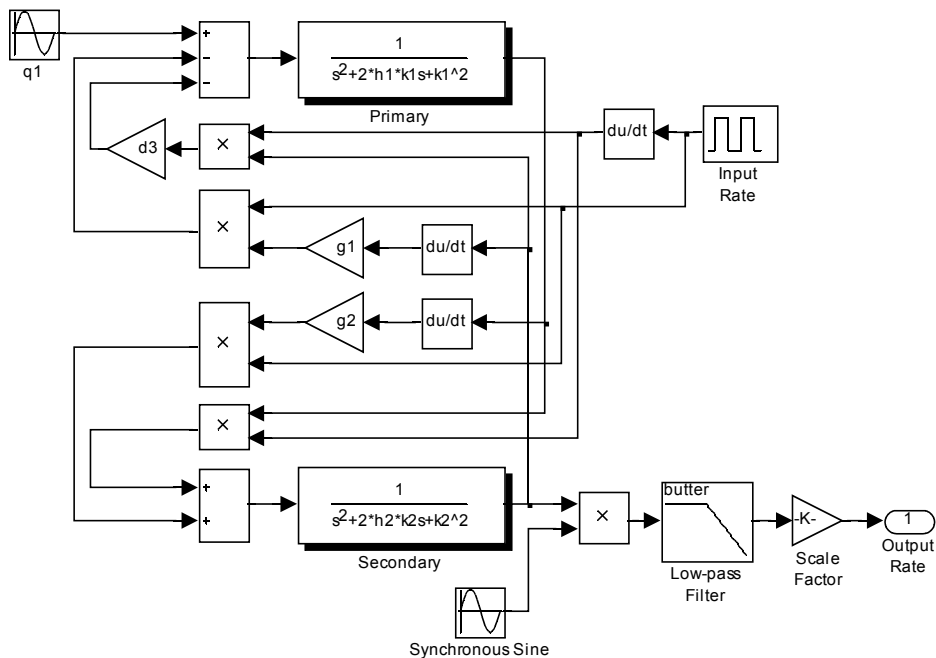


Fig. 3. Realistic CVG simulation model

Results of numerical simulations of the “white” disturbances filtering are shown in the figure 4.

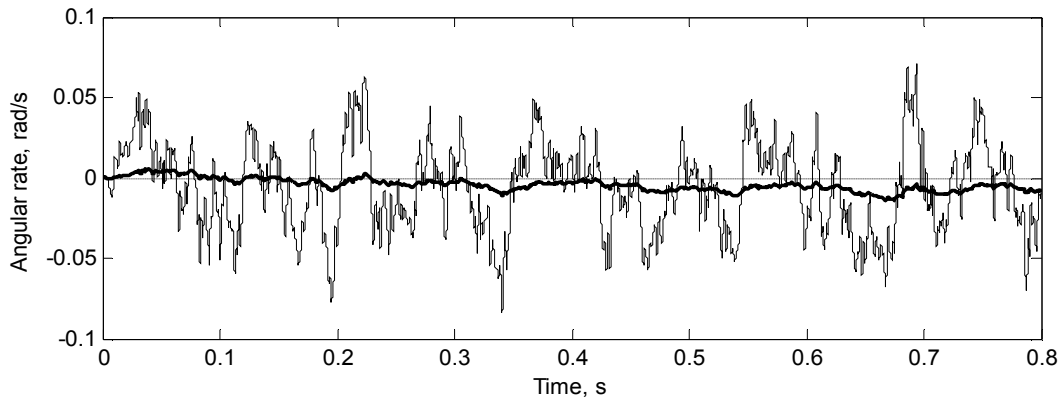


Fig. 4. Disturbances filtering simulations (thin – unfiltered, thick – filtered)

These simulations are performed for the high–level of disturbances ($\gamma=1$) and low bandwidth of the angular rate ($B=0.5$ Hz). When bandwidth of the angular rate is increased, disturbances filtering efficiency degrades.

Filtering efficiency

Let us study efficiency of the filtering as a function of the angular rate bandwidth B and disturbances–to–rate ratio γ . These dependencies are shown in the figures 5 and 6.

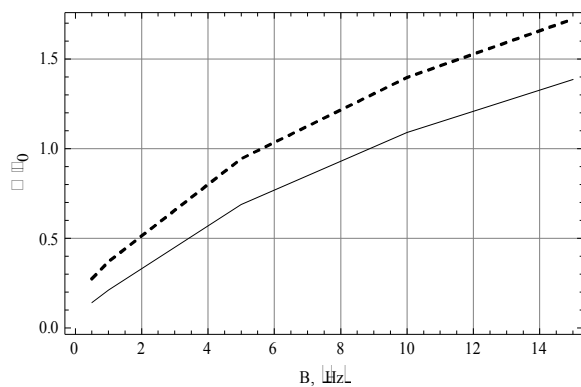


Fig. 5. “White” disturbances filtering efficiency

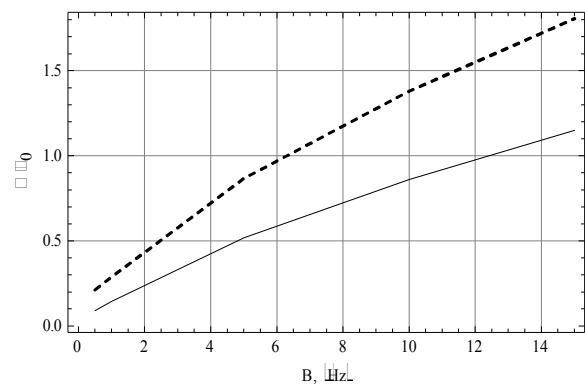


Fig. 6. “High–pass” disturbances filtering efficiency

Here solid lines correspond to the $\gamma=1$ and dotted line to $\gamma=0.5$. The lower level of the standard deviation ratio σ/σ_0 the better filtering quality. One should note, that when the standard deviation ratio higher than one, the filtering does not improve the quality of the angular rate measurements.

At the same time, while bandwidth of the angular rate lower than the bandwidth of the CVG, filters still can improve the characteristics of the sensors.

Conclusions

Presented above synthesis of the stochastic disturbances filters resulted in two static filters capable of improving the performances of Coriois vibratory gyroscopes in case of “white” and “high-pass” process noise. The latter has been demonstrated using explicit numerical simulations. The further analysis of the sensitivity of the filters performances in case of varying parameters of gyroscopes is viewed as a possible future development of the current research.

References

1. *Friedland B., Hutton M. F.* Theory and error analysis of vibrating-member gyroscope // IEEE Transactions on Automatic Control, no. 23, 1978, pp. 545–556.
2. *Lynch D.* Vibratory gyro analysis by the method of averaging // Proc. 2nd St. Petersburg Conf. on Gyroscopic Technology and Navigation, St. Petersburg, 1995, pp. 26–34.
3. *Apostolyuk V., Tay F.* Dynamics of Micromechanical Coriolis Vibratory Gyroscopes // Sensor Letters, Vol. 2, No 3–4, 2004, pp. 252–259.
4. *Apostolyuk V. A., Logeeswaran V.J., Tay F.E.H.* Efficient design of micromechanical gyroscopes // Journal of Micromechanics and Microengineering, Vol. 12, 2002, pp. 948–954.
5. *Apostolyuk V. A.* Theory and Design of Micromechanical Vibratory Gyroscopes // MEMS/NEMS Handbook (Ed: Cornelius T. Leondes), Springer, 2006, Vol.1, Chapter 6, pp. 173–195.
6. *Apostolyuk V.A.* Coriolis Vibratory Gyroscopes in Control Systems // Proc. of the IX Int. Conference “Avia–2009”, vol. 2, 2009, pp. 9.1–9.4.
7. *Leland R.* Mechanical Thermal Noise in Vibrating Gyroscopes // Proc. of the American Control Conference, June 25–27, 2001, pp. 3256–3261.
8. *Blokhin L.N., Burichenko M.Y.* Statistical Dynamics of Control Systems // NAU, Kiev, 2003, 208 p.